UNIVERSITY OF
BATH

University of Bath

Magnetoelectric doubling and mixing of electric and magnetic field frequencies in a layered multiferroic heterostructure

D.A. Burdin[1], N.A. Ekonomov[1], D.V. Chashin[1], Y.K. Fetisov[1] and S.N. Gordeev[2]

[1]MIREA - Russian Technological University, 119454 Moscow, Russia

[2] Department of Physics and Centre for Nanoscience & Nanotechnology, University of Bath, BA2 7AY, U.K.

Abstract

Nonlinear magnetoelectric effects in a disk-like heterostructure composed of a layer of amorphous ferromagnet (FeBSiC) mechanically coupled to a layer of piezoelectric ceramics (lead zirconate titanate) were studied both experimentally and theoretically. The structure was excited by alternating electrical and magnetic fields far from its acoustic resonance frequency. This induced changes in the magnetic induction within the heterostructure which were recorded using an electromagnetic coil. The experiments were performed for excitations with electric and magnetic fields up to 250 V/cm and 6 Oe, respectively, and bias permanent magnetic fields up to 60 Oe. For large excitation fields, a generation of the second harmonic and harmonics corresponding to the sum and difference frequencies were observed. The coefficient of the frequency doubling for the converse magnetoelectric effect and the coefficient of mixing of electrical and magnetic field frequencies were found to be $4.6 \cdot 10^{-6}$ G·cm^2/V^2 and $\sim 1 \cdot 10^{-2}$ G·cm/(Oe·V), respectively. A simple theoretical model qualitatively describing the experimental findings was proposed. It was shown that the nonlinearity in the converse magnetoelectric effect arises due to the nonlinear dependence of magnetic induction in the ferromagnetic layer on mechanical stress.

Keywords: multiferroic heterostructure, nonlinear magnetoelectric effect, piezoelectric effect, elastomagnetic effect, frequency mixing, frequency doubling.

1. Introduction

Magnetoelectric (ME) effects in planar multiferroic ferromagnet-piezoelectric (FM-PE) heterostructures are currently a subject of intense research due to their importance for the development of novel sensors of magnetic/electric field, radio-signal processing devices, and

magnetic memory [1-3]. ME effects in heterostructures arise because of a combination of the magnetoelectric and piezoelectric properties of the layers and due to the mechanical coupling between the layers. Normally these effects in planar structures significantly exceed that in homogeneous multiferroics. The direct ME effect manifests itself as the generation of an alternating electric field when the structure is excited by an alternating magnetic field, while the converse ME effect is responsible for producing an alternating magnetic field when the structure is excited by an alternating electric field.

By now, the characteristics of linear direct and converse ME effects in structures of various shapes with layers from various FM and PE materials have been studied in detail. In particular, it was demonstrated that the efficiency of the ME interaction depends on the frequencies of the excitation magnetic and electric fields, their magnitudes, the directions of permanent magnetic and electric fields applied to the heterostructure, the thickness of the layers and other factors [4,5]. It was also shown that the magnitude of the effects increases resonantly when the excitation frequency coincides with acoustic resonances in the structure [6].

A number of nonlinear effects were reported for the direct ME effect when a large-amplitude excitation magnetic field was applied to an FM-PE heterostructure. In particular, generation of harmonics [7,8], mixing of magnetic field frequencies [9-11], static deformation of the ferromagnet in an alternating magnetic field [12], suppression of the hysteresis of the ME effect [13] in multilayer structures were observed. The physical reason for the appearance of nonlinear direct ME effects is a nonlinear dependence of the magnetostriction of the FM layer $\lambda(H)$ on the magnetic field H [14].

It was demonstrated that both the amplitude and the field dependences of the generated harmonic at the excitation frequency are determined by the piezomagnetic coefficient of the FM layer, i.e. the first derivative of magnetostriction with respect to the field, $\lambda^{(1)} = \partial\lambda/\partial H$. The amplitudes of harmonics corresponding to the sum/difference and double frequencies are determined by the nonlinear piezomagnetic coefficient, i.e. the second derivative of magnetostriction, $\lambda^{(2)} = \partial^2\lambda/\partial H^2$ [14, 15].

The converse linear ME effect in composite multiferroic FM-PE structures of various compositions was investigated by several research groups [16-22]. At the same time, nonlinear converse ME effects have not been investigated in detail to date. Only an addition of frequency spectra for simultaneous excitation by magnetic and electric fields in a structure containing FM and PE films on a PE substrate [23], a modulation of the magnetic field generated by the electric field in the structure containing an FM film and two PE films on the silicon substrate [24, 25],

and mixing of magnetic field and electric fields in the structure containing a FM layer sandwiched between two PE layers [26] were observed. A possibility of manipulating the characteristics of the converse ME effect using a static electric field was also demonstrated [27]. Until today, the physical mechanism responsible for the appearance of nonlinearities in the converse ME effect in FM-PE heterostructures has not been elucidated. Still, there is no theory explaining, even qualitatively, the dependence of the characteristics of nonlinear converse ME effects on external static fields and the amplitudes of alternating excitation fields.

In this paper, we present experimental and theoretical studies of nonlinear converse ME effects, such as doubling and mixing of the frequencies of magnetic and electric fields in a model two-layer structure consisting of an amorphous ferromagnet FeBSiC and piezoelectric lead zirconate titanate (PZT). The first part of the article describes sample fabrication and the measurement procedures used. The second part presents experimental dependences for conversion efficiency of the fields on the strength of a permanent magnetic field and the amplitudes of the excitation fields. The third part contains a simple theory for harmonics generation and mixing of magnetic and electric fields in a two-layer structure. Finally, in the last part of the article, the physical mechanism of the converse nonlinear ME effects in multiferroic heterostructures is discussed.

2. Experimental details

The measurements were carried out on a disk-like structure of 16 mm in diameter, containing a 20 μm thick layer of amorphous ferromagnet FeBSiC (Metglas [28]) and a 200 μm thick layer of lead zirconate titanate ceramics $Pb_{0.48}Sr_{0.52}TiO_3$ (PZT), schematically depicted in Fig. 1. The FM layer was initially annealed at 200° C for 30 minutes to eliminate any anisotropy. The saturation magnetostriction of the FM layer was $\lambda_S \approx 21 \cdot 10^{-6}$ in the saturation field $H_S \approx 100$ Oe. The PZT layer was poled perpendicular to its plane, and its surfaces were covered with ~ 2 μm thick Ag electrodes. The disk capacity at 10 kHz was 17 nF and the piezoelectric modulus $d_{31} = 175$ pm/V. The Metglas and PZT discs were bonded to each other with an epoxy glue.

During the measurements, the sample was placed inside two mutually orthogonal flat electromagnetic coils, whose axes were parallel to the sample plane (see Fig. 1). Each coil contained $N=120$ turns of a 0.2 mm wire. The internal coil was used to excite the ME effect in the structure by an alternating magnetic field $h\cos(2\pi f_m t)$ with a frequency $f_m = 10$ Hz - 100 kHz and an amplitude up to $h = 5$ Oe. For the electrical excitation of the ME effect in the structure, a voltage $U_2(f_e)$ with an amplitude of up to 5 V was applied to the electrodes of the PZT disk,

which created an electric field $e \cdot \cos(2\pi f_e t)$ in the disk with a frequency $f_e = 10$ Hz -100 kHz and an amplitude up to $e = 250$ V/cm. The external electromagnetic coil was used to record changes of magnetic induction in the structure. The orthogonality between the axes of the excitation and recording coils allowed to minimize any direct electromagnetic interference and ensured high sensitivity of signal detection. In addition, a static magnetic field $H = 0 - 100$ Oe was applied to the structure along the axis of the excitation coil using Helmholtz coils. The magnetic field was measured with an accuracy of 0.1 Oe using the LakeShore 421 Gaussmeter. Amplitude-frequency characteristics, $u(f)$, of the direct (excited by h-field) and converse (excited by e-field) ME effects were recorded for frequencies in the range of 0-12 kHz. Voltage spectra generated by the receiving coil under excitation of the sample with magnetic or/and electrical field of a fixed frequency, were assessed using FFT Spectrum Analyzer SR770. Amplitudes of the spectral components $u(f)$ as a function of applied bias field H and excitation magnetic, h, and electric, e, fields were recorded.

3. Experimental results

First, the amplitude-frequency characteristics of the direct and inverse ME effects in the described disk-like structure were measured for small-amplitude excitation fields. In Fig. 2, the solid line shows the frequency dependence of the voltage generated by the PZT layer when the structure is excited by an alternating magnetic field of amplitude $h = 1$ Oe while frequency varies in the range of 0-12 kHz. The dashed line in Fig. 2 shows the corresponding frequency dependence for the voltage generated by the receiving coil when the structure is excited by an alternating electric field of amplitude $e = 12.5$ V / cm. It is seen that the amplitude-frequency characteristics of the direct and inverse ME effects qualitatively agree with each other. Both dependences have resonance peaks at ~ 3.9 kHz and ~ 5.5 kHz. Estimates of the frequencies of the peaks, using the formulae for a free disk [29] with parameters of the layers as in our experiment, show that these peaks correspond to excitation of the lowest modes for bending vibrations in the structure.

At the second stage, frequency spectra of the voltage response generated by the layered structure that was excited by alternating fields with fixed frequencies were investigated. All measurements were performed in a non-resonant mode. For this, the frequencies of the excitation fields were chosen equal to $f_m = 10$ kHz and $f_e = 7$ kHz, so that neither the frequencies themselves nor their harmonics coincided with the frequencies of acoustic resonances in the

4

structure. This enabled us to get rid of any resonance phenomena thus significantly simplifying interpretation of the experimental results.

Experiments with the FM-PE heterostructure depicted in Fig. 1 showed that the measured voltage response u is strongly dependent on the method of excitation and the magnitude of the applied bias magnetic field, H. Figure 3 shows typical frequency spectra of the voltage generated by the receiving coil for $H \approx 14$ Oe and for three different methods of excitation. When the structure was excited by the electric field (Fig. 3a) with the frequency of $f_e = 7$ kHz and amplitude $e = 100$ V/cm, the corresponding spectrum of the output voltage contained the fundamental harmonic u_e and two higher harmonics with frequencies 14 kHz and 21 kHz. When the structure was excited by the magnetic field (Fig. 3b) with the frequency of $f_m = 10$ kHz and amplitude of $h = 1$ Oe, only the fundamental, u_m, and double-frequency harmonic, u_{2m}, were detected. Finally, when electric and magnetic fields were applied simultaneously (Fig. 3c), components with the difference, f_m-f_e, and sum, f_m+f_e, frequencies appeared in the frequency spectrum, in addition to the fundamental and higher harmonics of the excitation fields. This proves the mixing of the frequencies of magnetic and electric fields in the sample.

Figure 4 shows amplitudes of spectral components as a function of bias magnetic field H when the structure was excited by both magnetic and electrical fields. As can be seen in Fig. 4a, the fundamental harmonic u_m initially increases linearly with the field, reaching its maximum at $H_m \sim 15$ Oe, and then gradually decreases as the FM layer becomes saturated. The $H_m \approx 15$ Oe field corresponds to the maximum of the piezomagnetic coefficient $\lambda^{(1)}(H)$ of the FM layer of the structure [30]. The u_e component, corresponding to the excitation frequency $f_e = 7$ kHz of the electric field, also initially increases linearly with the magnetic field up to $H = H_m$, and then steadily decreases practically to zero (see Fig. 4b). The amplitude of the u_{m-e} component (Fig. 4c) corresponding to the difference frequency $f_{m-e} = 3$ kHz is largest in the region of small fields, then decreases practically to zero at $H \sim H_m$. After that it initially grows, reaching its second maximum, and then asymptotically reduces to zero with increasing H. The u_{m+e} component (Fig.4d), corresponding to the sum frequency $f_{m+e} = 17$ kHz, has a similar dependence on H. It is worth mentioning that the amplitude of this spectral component is approximately 5 times greater than u_{m-e}. This is due to the employed method of recording the output signal using a coil, in which the amplitude of the generated voltage is proportional to the frequency. Finally, the amplitude of harmonic u_{2e} (Fig. 4e), corresponding to the double frequency, f_{2e}, of the electric field, initially increases from zero, then drops back to zero at H_m. After that, it grows, reaches its second maximum and then gradually decreases to zero with increasing H.

Figure 5 shows dependences of harmonic amplitudes u_{m+e} and u_{m-e}, corresponding to the sum and difference frequencies, on the excitation electric field, e, for the constant amplitude of magnetic field $h = 1$ Oe (Fig. 5a), and on the excitation magnetic field h, for the constant amplitude of electric field $e=100$ V/cm (Fig. 5b). The dashed lines in the figures are linear approximations to the data. It can be seen that the amplitudes of both harmonic components grow linearly with increasing e and h. Similar to what was mentioned earlier, the response corresponding to the sum frequency (u_{m+e}) is ~ 5 times larger of that for the difference frequency (u_{m-e}). Figure 5c shows the dependence of the harmonic amplitude u_{2e} corresponding to the double frequency $2f_e$ of the electric field on the amplitude of excitation field e at $H \approx 7.5$ Oe. The obtained results can be approximated by a quadratic function (dashed curve). Similarly, the dependence of the harmonic amplitude corresponding to the double frequency, $2f_m$, of the magnetic field (not shown in the figure) on the amplitude of the excitation field at $h < 3$ Oe was also found to be well described by a quadratic function, confirming the earlier findings [14].

4. Theory for fields mixing

In order to explain the observed experimental results, we used the approach developed in Ref. 14. To demonstrate our findings, let us first consider the effect of static magnetic and electric fields, and then discuss excitations induced by alternating magnetic and electric fields on an example of the disk-like ME-PE heterostructure depicted in Fig. 1. Here the magnetic field $H+h$ in the FM layer is directed along the x-axis and the electric field e in the PE layer along the z-axis. We assume that $h \ll H_s$ and $e \ll E_s$, where H_s and E_s are the saturation fields of the FM and PE layers, respectively. In this case, both the deformation in the FM layer caused by magnetic field H and the deformation in the PE layer caused by electric field e can be approximated by linear functions of the corresponding fields. Also, for simplicity, let us consider a one-dimensional problem when all deformations and magnetic fields are directed along the x-axis. Then, the mechanical strain S, the mechanical stress T, the magnetic field intensity h in the FM layer and the electric field e in the PE layer are linked by the following relationships [31]:

$$S_1^m = s_{11}^m T_{m1} + q_{11} h_1 , \tag{1}$$

$$S_1^p = -s_{11}^p T_{p1} + d_{31} e_3 ,$$

$$B = B_0(H) + b(H, T_{m1}) ,$$

where we used indices 1, 2 and 3 to indicate x, y and z components, respectively, to keep our notations in accord with those in the literature. The indices "m" and "p" correspond to the FM

and PE layers, respectively, q_{11} is the piezomagnetic coefficient of the FM layer, $q_{11} = \lambda^{(1)}(H) = \partial\lambda/\partial H$, $\lambda(H)$ is the magnetostriction, d_{31} is the piezo-modulus of the PE layer, $s_{11}^m = 1/Y_m$ and $s_{11}^p = 1/Y_p$ are the compliance coefficients, where Y_m and Y_p are Young's moduli of the FM and PE layers, respectively. The last equation in (1) describes the relationship between the total magnetic induction in the FM layer with the induction created by a constant magnetic field $B_0(H)$ and additional induction $b(H, T_{m1})$ arising due to solely the mechanical stress, T_{m1}.

Continuity conditions for the deformations at the layers interface and the equilibrium condition of the structure along the x-axis have the form

$$S_1^m = S_1^p \quad \text{и} \quad T_{p1}a_p - T_{m1}a_m = 0, \tag{2}$$

where a_p and a_m are the thicknesses of the PE and FM layers, respectively.

Solving the equations (1) with conditions (2), we obtained the following expression for the mechanical stress in the FM layer of the structure

$$T_{m1} = \frac{d_{31}e_3 - q_{11}h_1}{s_{11}^m a_p + s_{11}^p a_m} a_p. \tag{3}$$

It can be seen from Eq. (3) that the mechanical stress in the FM layer is created jointly by magnetic field h_1 and electric field e_3. This mechanical stress, due to the elastomagnetic effect (inverse magnetostriction or Villari effect), causes the appearance of an additional magnetic induction in the FM layer of the structure along the x-axis [32,33]. As will be shown below, a dependence of magnetic induction $b(H, T_{m1})$ on mechanical stress is the physical reason for the appearance of the linear and nonlinear converse ME effects of mixing the frequencies of the magnetic and electric fields and doubling the frequency of the electric field in the heterostructure.

Next we consider the sample response to variable fields and find the expression for magnetic induction in the FM layer. Let a magnetic field of the form $h\cos(2\pi f_m t)$ with a frequency f_m act on the structure, and an electric field $e\cos(2\pi f_e t)$ with a frequency f_e be generated in the PE layer (for simplicity, the indices of the fields h and e are further omitted). Expanding the magnetic induction b into a Taylor series near T_0 and substituting harmonic fields $h(f_m)$ and $e(f_e)$ into the expansion, after transformations one can obtain the following relation for the time-dependent induction, expressed as a sum of five terms:

$$b(t) = \frac{a_p}{s_{11}^m a_p + s_{11}^p a_m} b^{(1)} q_{11} h \sin(2\pi f_m t) + , \tag{4a}$$

7

$$+ \frac{a_p}{s_{11}^m a_p + s_{11}^p a_m} b^{(1)} d_{31} e \sin(2\pi f_e t) + \tag{4b}$$

$$+ \frac{1}{2} \left[\frac{a_p}{s_{11}^m a_p + s_{11}^p a_m} \right]^2 b^{(2)} q_{11}^2 h^2 \sin(4\pi f_m t) + \tag{4c}$$

$$+ \frac{1}{2} \left[\frac{a_p}{s_{11}^m a_p + s_{11}^p a_m} \right]^2 b^{(2)} d_{31}^2 e^2 \sin(4\pi f_e t) + \tag{4d}$$

$$+ \frac{1}{4} \cdot \left(\frac{a_p}{s_{11}^m a_p + s_{11}^p a_m} \right)^2 b^{(2)} q_{11} d_{31} h e \cdot \left[\sin 2\pi (f_m + f_e)t + \sin 2\pi (f_m - f_p)t \right], \tag{4f}$$

where $b^{(1)} = \partial b / \partial T_{m1}$ is the elastomagnetic coefficient and $b^{(2)} = \partial^2 b / \partial T_{m1}^2$ is the nonlinear elastomagnetic coefficient. Terms (4a) and (4b) describe the linear direct and converse ME effects, i.e. generation of the magnetic field with the frequencies of the excitation magnetic and electric fields, respectively. The amplitudes of these components are proportional to the amplitudes of the excitation magnetic field h and excitation electric field e. The dependences of the amplitudes of the fundamental harmonics on a constant field H are determined by the field dependence of the coefficient $b^{(1)}(H)$. Terms (4c) and (4d) describe the generation of second harmonics by magnetic and electric fields, respectively. The amplitudes of the harmonics depend quadratically on the amplitudes of the excitation fields. The form of the field dependences of the amplitudes of the second harmonics is determined by the field dependent coefficient $b^{(2)}(H)$. Term (4f) describes the mixing of the frequencies of the magnetic and electric fields. The amplitude of this term is a linear function of the product of the amplitudes of the electric and magnetic fields. It follows from Eq. 4 that the linear and nonlinear converse ME effects in the composite structure take place only when the magnetic induction in the FM layer depends on mechanical stress and the expansion coefficients are nonzero, i.e. $b^{(1)} \neq 0$ and $b^{(2)} \neq 0$.

5. Elastomagnetic effect

It follows from Eq. 4 that characteristics of converse linear and nonlinear ME effects depend on the elastomagnetic characteristics of the FM layer of the structure, specifically, on first, $b^{(1)}(H,T)$, and second, $b^{(2)}(H,T)$, derivatives of magnetic induction b with respect to mechanical stress T. The function $b(H,T)$ for converse ME effect plays the same role as the dependence of magnetostriction of the FM layer on field, $\lambda(H)$, for direct ME effect [14, 15].

To establish the form of the function $b(H,T)$, static elastomagnetic characteristics of a Metglas tape were measured as it was stretched by an external stationary force. This was performed by placing a Metglas tape (50 mm long, 4 mm wide and 20 μm thick) inside a 25 mm long vertical coil that had $N_2 = 1000$ turns and a cross section of $A = 16$ mm^2. A constant magnetic field $H = 0\text{-}50$ Oe was applied parallel to the coil axis. The upper end of the tape was fixed, while a mass of $m = 0\text{-}100$ g was hung to the free lower end. This allowed creating tensile mechanical stresses with values of $T_m = 0 - 12.5$ MPa in the Metglas tape. Coil's inductance was measured using an ammeter-voltmeter with an accuracy of 0.1% at 1 kHz. The coil's inductance was $L_0 = 1.9$ mH in the unloaded state but increased to $L = 16.5$ mH when the sample was placed in it.

Induction of magnetic field B in the FM layer was determined from the measured coil inductance L as follows. Inductance of a long unloaded coil is given by the formula $L_0 = n^2 V$, whereas its inductance with an FM sample inside it is $L = \mu \cdot (A_0 / A) \cdot n^2 V$, where μ is the differential magnetic permeability of the FM sample, A_0/A the coil filling factor, A_0 the cross-sectional area of the FM sample, A the coil cross-section area, and n the number of coil turns per unit length. Using these formulae, one can get induction of the magnetic field inside the FM layer in the following form:

$$B(H,T) = \int_0^H \mu(H,T)dH = \frac{A}{A_0 L_0} \int_0^H L(H,T)dH . \tag{5}$$

This relation enabled us to construct the function $B(H,T)$ by measuring the coil's inductance with the sample in it as a function of H for various mechanical stresses T followed by integration the obtained functional dependences over the field.

Figure 6 shows the measured field dependences of the coil's inductance loaded with the Metglas tape for 20 different mechanical stresses in the range of $T = 0 - 12.5$ MPa. The inductance of the coil decreased from $L = 16.5$ mH to $L_0 = 1.9$ mH with increasing magnetic field. It can be seen that for $H = H_0 \approx 4$ Oe, mechanical stress does not affect inductance of the structure, while for $0 < H < H_0$, inductance increases and for $H > H_0$ decreases with increasing T. Integrating these curves numerically, magnetization curves $B(H, T)$ for various stresses were obtained. After that, the magnetization curve without load $B_0(H,T=0)$ was subtracted from each magnetization curve. Figure 7 shows the additional magnetic induction $b(H,T) = B(H, T) - B_0(H,T=0)$, produced by only mechanical stresses in the Metglas layer, as a function of two variables. The pronounced roughness of the $b(T)$ dependence observed at fields above 15 Oe is due to measurement errors that were further enhanced by the numerical integration process.

9

Analysis of curves representing cross-sections of the $b(H,T)$ surface in Fig. 7 for various T = const values shows that for small T (< 1 MPa) induction b initially increases from zero with increasing H, then, after reaching its maximum at $H_m \approx 4$ Oe, asymptotically decreases to zero as the FM layer becomes saturated. For large T = const values these dependences become a bit different. The induction b initially also grows approximately linearly with increasing H, reaching its maximum at the same $H=H_m$, then decreases to a minimum at $H \approx 16$ Oe and after that rises again.

A similar analysis of H=const cross-sections shows that for all H values the additional induction b increases monotonically with increasing stress T. Our estimations confirmed that in the disk structure that was studied, mechanical stress in the Metglas layer did not exceed ~ 0.5 MPa. Therefore, the behaviour of curves $b(T)$ in the low mechanical stress region, $T < 0.5$ MPa, is of most interest. Figure 8 shows the dependence of the elastomagnetic coefficient $b^{(1)}(H)$ corresponding to the initial part of the $b(H,T)$ data in Fig. 7. It can be seen that $b^{(1)}$ starts to increase from zero at $H = 0$, then reaches its maximum value of $b^{(1)}(H_m) \approx 250$ G/MPa at $H_m \approx 4$ Oe, and after that decreases steadily with increasing H.

6. Discussion

Comparing the experimental results shown in Figs 3-5 and 7-8 with the theoretical predictions given by Eq.(4), the following conclusions can be drawn:

1) For the direct linear ME effect, the dependence of harmonic amplitude u_m at frequency f_m (Fig. 4a) on the static field H is described qualitatively correctly by Eq. (4a) and is determined by the field dependence of the elastomagnetic coefficient $b^{(1)}(H)$, shown in Fig.8, and piezomagnetic coefficient $q_{11}(H)$ of the FM layer [14].

2) For the converse linear ME effect, the dependence of the harmonic amplitude at frequency f_e (Fig. 4b) on H is described qualitatively correctly by Eq. (4b) but, in this case, is determined by the elastomagnetic coefficient $b^{(1)}(H)$ only.

3) For the doubling of the electric field frequency in the converse ME effect (Fig. 4e), the dependence of the harmonic amplitude on the field H is determined by the field dependence of the nonlinear elastomagnetic coefficient $b^{(2)}(H)$. Similarly, for the magnetic and electric fields frequencies mixing in the converse ME effect, the dependence of the harmonic amplitudes (Fig. 4c and 4d) on the field H is determined by the field dependence of the nonlinear elastomagnetic coefficient $b^{(2)}(H)$ too. Summarising, it can be concluded that Eqs (4) give a realistic qualitative description of all our experimental findings presented in Figs 3-5 and 7-8. However, we have

found that the accuracy of the obtained experimental data was not high enough to get a reliable quantitative comparison with the theory.

4) The theoretical prediction for the field $H_m \approx 14$ Oe, corresponding to both the conversion maximum for the linear converse ME effect and the minimum of harmonic amplitudes for nonlinear ME effects in the Metglas-PZT structure (Fig. 3), turned out to be higher than the experimentally measured value of 4 Oe corresponding to the maximum of the elastomagnetic coefficient $b^{(1)}$ (Fig. 8) in the Metglas tape. The discrepancy is believed to be solely due to the difference in the magnitude of demagnetization effects in the samples that had substantially different dimensions [34]. For the same internal field, the characteristic field H_m for a 50 mm long Metglas tape is significantly smaller than for a Metglas disk of 16 mm in diameter.

Let us estimate the conversion coefficients for linear and nonlinear converse ME effects in the structure studied, $\alpha_B^{(1)} = \delta B_1 / e$ and $\alpha_B^{(2)} = \delta B_2 / e^2$, where δB_1 and δB_2 are the amplitudes of the first and second harmonics of magnetic induction, respectively, produced by the alternating electric field with amplitude e. The values of δB can be found from the electromagnetic induction law, $u = N \cdot \delta B \cdot A_0 \cdot 2\pi f_e$, where u is the amplitude of the harmonic generated by the measuring coil, and f_e is the frequency of the excitation field. Here A_0 should be taken as the cross-section of the FM disk ~ 0.3 mm^2 since the field induction varies only within the FM layer. Substituting parameters corresponding to the data in Fig. 4a for $H = 15$ Oe at $e = 100$ V/cm into the formula for the induction law, we found $\delta B_1 \approx 19$ G and the coefficient of linear ME conversion $\alpha_B^{(1)} \approx 0.19$ G·cm/V. Using the data in Fig. 4c for $H = 7.5$ Oe and $e = 100$ V/cm, we obtained $\delta B_2 \approx 0.05$ G and the coefficient of nonlinear ME conversion $\alpha_B^{(2)} \approx 4.6 \cdot 10^{-6}$ G·cm^2/V^2.

The obtained coefficient of linear ME conversion in the case of the Metglas-PZT structure is smaller than the conversion coefficients of 0.27 G·cm/V for a PZT-Ni structure [17] and 30 G·cm/V for a Metglas-PMN-PT structure [21], where the effect was observed in the resonance mode. The efficiency of frequency doubling in the Metglas-PZT structure in the case of the converse ME effect is of the order of magnitude of the efficiency of frequency doubling $3 \cdot 10^{-6}$ G·cm^2/V^2 in the Metglas-electrostrictor structure, where the second harmonic is generated due to nonlinear effects in the electrostriction layer [35].

The same method can be used to estimate the efficiency of magnetic and electric field frequency mixing in the case of the converse ME effect in the structure studied. Using the data in Fig. 3a for $H \approx 7.5$ Oe, we obtained changes in the magnetic induction of $\delta B_{m+e} \approx 0.96$ G and $\delta B_{m-e} \approx 1.1$ G. The efficiency of signal generation with the sum frequency

$\alpha_{m+e}^{mix} = u_{m+e} / he \approx 0.96 \cdot 10^{-2}$ G·cm/(Oe·cm) is approximately equal to the efficiency of signal generation with the difference frequency $\alpha_{m-e}^{mix} = u_{m-e} / he \approx 1.1 \cdot 10^{-2}$ G·cm/(Oe·cm). Thus, the efficiency of frequency mixing is weakly dependent on frequencies of magnetic and electric fields, similar to the case of the direct ME effect [11].

Concerning the accuracy of the experimental data, it should be noted that the use of orthogonal coils for both magnetic excitation of the ME effect and recording of changes in magnetic induction actually undervalues the measured efficiency of field mixing in the composite structure due to Poisson effect. In addition, the orthogonality of the coils can affect the form of the field dependences $u(H)$ in Fig. 4 in the region of small fields $H < H_m$.

The coefficient for the converse ME effect can also be estimated, using Eq. (4f), from the experimentally obtained elastomagnetic coefficient $b^{(1)} \approx 250$ G/MPa, the known piezomagnetic coefficient $q \approx 1 \cdot 10^{-6}$ Oe^{-1} for the Metglas layer [14], and Young moduli of the layers in the structure, i.e. $Y_m = 10.6 \cdot 10^{10}$ N/m^2 and $Y_p = 7 \cdot 10^{10}$ N/m^2. These calculations give $\delta B_1 \approx 25$ G and $\delta B/e \approx 0.25$ G cm/V. So, the calculated coefficient of the converse linear ME transformation reasonably agrees with the measured value (0.19 G·cm/V) thus confirming the validity of the theoretical model used.

The results of our investigations open up new prospects for improving characteristics of ME sensors for detection of slow varying (1-100 Hz) magnetic fields [9,10,36]. In such sensors, the frequency of the measured field is mixed with the frequency of an additional (modulating) magnetic field and the information about the measured field is transferred to the acoustic resonance frequency thus improving the signal-to-noise ratio. However, the modulating magnetic field required for that is usually produced by electromagnetic coils, which consume a lot of energy and are not technologically easy to manufacture. Instead, as shown above, it is achievable to mix the frequency of the field that needs to be measured with the frequency of an alternating electric rather than magnetic field, which is both energetically and technologically more favourable. In addition, very often the inductance of the coils limits from above the frequency of the modulating magnetic field, which in turn imposes a restriction on dimensions of the sensor, since its resonance frequency is inversely proportional to its size. The use of structures with electrical excitation would allow to increase the operating frequency of ME sensors up to ~1 MHz, according to our estimations, and reduce their size by an order of magnitude.

7. Conclusions

In the work, the ME effects of doubling the frequency of the electric field and mixing the frequencies of magnetic and electric fields in a composite multiferroic structure containing a mechanically bonded layer of an amorphous ferromagnet FeBSiC and a layer of piezoceramics PZT were experimentally investigated. It was shown that the converse linear and nonlinear ME effects in such composite structures arise due to the dependence of magnetic induction on mechanical stress in the ferromagnetic layer (elastomagnetic effect or inverse magnetostriction).

The physical mechanism of the converse nonlinear ME effects in multiferroic heterostructures have been discussed and a simple theory describing the converse ME effects in composite structures has been developed. It is demonstrated that the constructed theory gives a good qualitative description of the experimental observations. Our findings can be instrumental in manufacturing magnetic field sensors and devices for processing low-frequency radio signals based on multiferroic heterostructures.

Figure captions

Fig. 1. Schematic of the disk-like piezoelectric-ferromagnetic heterostructure.

Fig. 2. Amplitude-frequency characteristics for the direct (solid line) and converse (dashed line) ME effects in the disk Metglas-PZT heterostructure at H=14 Oe.

Fig. 3. Frequency spectra of the voltage generated by Metglas-PZT heterostructure when excited by: (a) magnetic field, (b) electric field, (c) magnetic and electric fields at the same time. Bias magnetic field is $H = 13$ Oe.

Fig. 4. Amplitudes of spectral components of voltage response versus bias magnetic field H in the case of simultaneous excitation of the heterostructure by magnetic (h=1 Oe, f_{m} =10 kHz) and electric ($e = 100$ V/cm, $f_{\mathrm{e}} = 7$ kHz) fields.

Fig. 5. Dependences of amplitudes of harmonics with difference and sum frequencies on: (a) amplitude of electric field e for $h = 1$ Oe and (b) amplitude of magnetic field h for $e = 100$ V/cm and $H = 3$ Oe. (c) The amplitude of the $2f_{\mathrm{e}}$ harmonic versus amplitude of electric field e for $H = 7.5$ Oe.

Fig. 6. Dependence of inductance L of the coil loaded with the FM tape on bias magnetic field H for different mechanical stresses T.

Fig. 7. Magnetic induction b in the Metglas layer as a function of magnetic field H and mechanical stress T.

Fig. 8. Dependence of linear elastomagnetic coefficient $b^{(1)}$ on magnetic field H for Metglas tape for low mechanical stresses ($T \approx 0$).

References

1. Y. Wang, J. Li, D. Wiehland, Mater. Today, **17**, 269 (2014).

2. M.M. Vopson, Crit. Rev. Solid State and Mater. Science, **40**, 223 (2015).

3. J-M. Hu, L.-O. Chen, C-W. Nan, Adv. Mater., **28**, 15 (2016).

4. C.-W. Nan, M.I. Bichurin, S. Dong, D. Wiehland, G. Srinivasan, J. Appl. Phys. **103**, 031101 (2008).

5. H. Palneedi, V. Annapureddy, S. Priya, J. Ryo, Actuators, **5**, 9 (2016).

6. M.I. Bichurin, D.A. Filippov, V.M. Petrov, V.M. Laletin, N. Paddubmaya, G. Srinivasan G Phys. Rev. **B68,** 132408 (2003).

7. K.E. Kamentsev, Y.K. Fetisov, G. Srinivasan, Appl. Phys. Lett., **89**, 145210 (2006).

8. W. Zhang, G. Yin, J. Cao, J. Bai, F. Wei, Appl. Phys. Lett. **100,** 032903 (2012).

9. L. Shen, M. Li, J. Gao, Y. Shen, J.F. Li, D. Viehland, X. Zhuang, M. L. Sing, C. Cordier, S. Saez, C. Dolabdjian, J. Appl. Phys., **119**, 114510 (2011).

10. R. Jahns, H. Greve, E. Woltermann, E. Quandt, R. Knochel, Sens. Act. A **183**, 16 (2012).

11. D.A. Burdin, D.V. Chashin, N.A. Ekonomov, Y.K. Fetisov, L.Y. Fetisov, G. Sreenivasulu, G. Srinivasan J. Appl. Phys. **113**, 033902 (2013).

12. D.A. Burdin, D.V. Chashin, N.A. Ekonomov, Y.K. Fetisov, J. Magn. Mag. Mater., **406**, 217 (2016).

13. D.A. Burdin, D.V. Chashin, N.A. Ekonomov, L.Y. Fetisov, Y.K. Fetisov, J. Magn. Mag. Mater., **449**, 152 (2018).

14. D.A. Burdin, D.V. Chashin, N.A. Ekonomov, L.Y. Fetisov, Y.K. Fetisov, G. Sreenivasulu, G. Srinivasan, J. Magn. Mag. Mater., **358-359**, 98 (2014).

15. L.Y. Fetisov, D.A. Burdin, N.A. Ekonomov, D.V. Chashin, J. Zhang, G. Srinivasan, Y.K. Fetisov, J. Phys. D: Appl. Phys, **51**, 154003 (2018).

16. Y. Jia, S.W. Or, H.L Chan, X. Zhao, H. Luo, Appl. Phys. Lett., **88**, 2429902 (2006).

17. Y.K. Fetisov, V.M. Petrov, G. Srinivasan, J. Mater. Res., **22**, 2074 (2007).

18. C. Popov, H. Chang, P.M. Record, E. Abraham, R.W. Whatmore, Z. Huang, J. of Electroceramics, 20, 53 (2008).

19. Y. Chen, J. Gao, T. Fitchorov, Z. Cai, K.S. Ziemer, C. Vittoria, V.G. Harris, Appl. Phys. Lett., 94, 082504 (2009).

20. Y.K. Fetisov, K.E. Kamentsev, D.V. Chashin, L.Y.Fetisov, G. Srinivasan, J. Appl. Phys., **105**, 123918 (2009).

21. H.C. Huan, L.Y. Wang, S.C. Ma, Y.X.Zheng, Q.Q. Cao, D.H. Wang, Y.W. Du, Appl. Phys. Lett., **98**, 052505 (2011).

22. B.Tong, X.F., Yang, J. Ouyang, G.Q. Lin, S. Chen, J. All. Comp., **563**, 51 (2013).

23. L.Y. Fetisov, D.V. Chashin, Y.K. Fetisov, A.G. Segalla, G. Srinivasan, J. Appl. Phys., **112**, 014103 (2012).

24. P. Hayes, S. Salzer, J. Reermann, E. Yarar, V. Robisch, A. Piorra, D. Meyners, M. Hoft, R. Knochel, G. Schmidt, E. Quandt, Apppl. Phys. Lett., **108,** 182902 (2016).

25. P. Hayes, V. Schell, S. Salzer, D. Burdin, E. Yarar, A. Piorra, Y.K Fetisov, E. Quandt, J. Phys. D: Appl. Phys., 51(35), 354002 (2018),

26. P. Li, L. Bian, Y. Wen, X. Ji, T. Han, Y. Wang, Int. Mag. Conf., 23-27 April 2018, Singapore, Digest Book, p. 106.

27. H.-M. Zhou, H. Liu, Y. Zhou, W.-W. Hu, AIP Adv. **6**, 125016 (2016).

28. https://metglas.com/magnetic-materials/

29. S. Timoshenko, *Vibration Problems in Engineering*, New York: D. Van Nostrand, 1961, p. 431.

30. Y.X. Liu, J.G. Wan, J.M. Liu, C. W. Nan, J. Appl. Phys., **94**, 5118 (2003).

31. L.D. Landau and E.M. Lifshits, *Electrodynamics of Continuous Media* (New York: Pergamon) 1984.

32. J.M. Barandiaran, J. Gutierrez, A. Garda-Arribas, Phys. Stat. Solidi A, **208**, 2258 (2011).

33. P. Svec Sr, R. Szewczyk, J. Salach, D.Jackiewicz, P. Svec, A. Bienkowski, J. Hosko, J. Electr. Eng., **65**, 259 (2014).

34. M.P. Silva, P. Martins, A. Lasheras, J. Gutierrez, J.M. Barandiaran, S. Lanceros-Mendez, J. Magn. Mag. Mater., **377**, 29 (2015).

35. D.V. Saveliev, Y.K. Fetisov, D.V. Chashin, L.Y. Fetisov, D.A. Burdin, N.A. Ekonomov, J. Magn. Mag. Mater., **466**, 219 (2018).

36. J. Petrie, D. Viehland, D. Gray, S. Mandal, G. Sreenivasulu, G. Srinivasan, A.S. Edelstein, J. Appl. Phys., **110**, 124506 (2011).
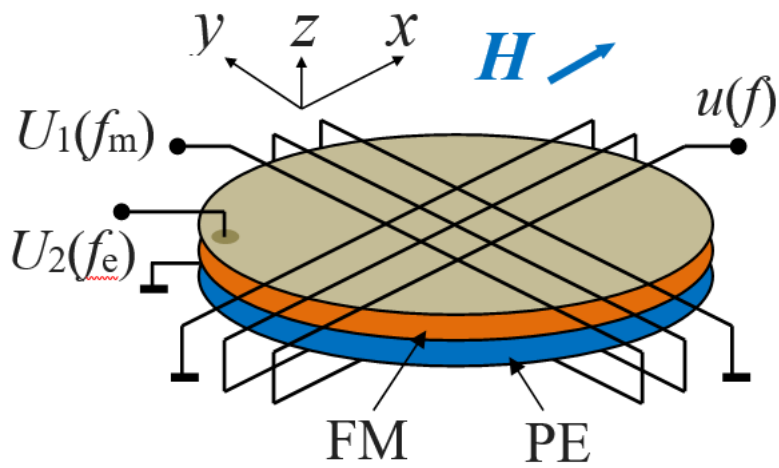
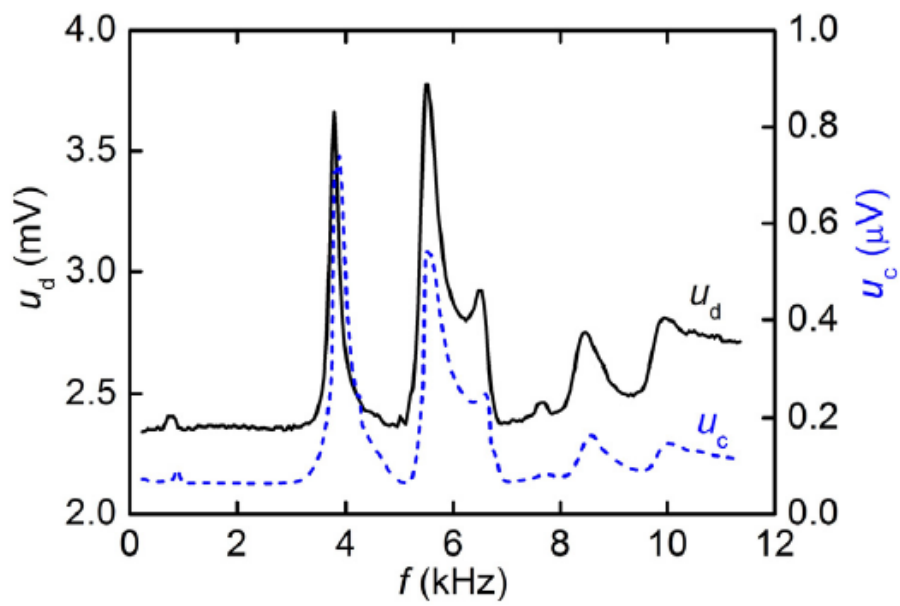Fig. 1. Schematic of the disk-like piezoelectric-ferromagnetic heterostructure.

Fig. 2. Amplitude-frequency characteristics for the direct (solid line) and converse (dashed line) ME effects in the disk Metglas-PZT heterostructure at H=14 Oe.
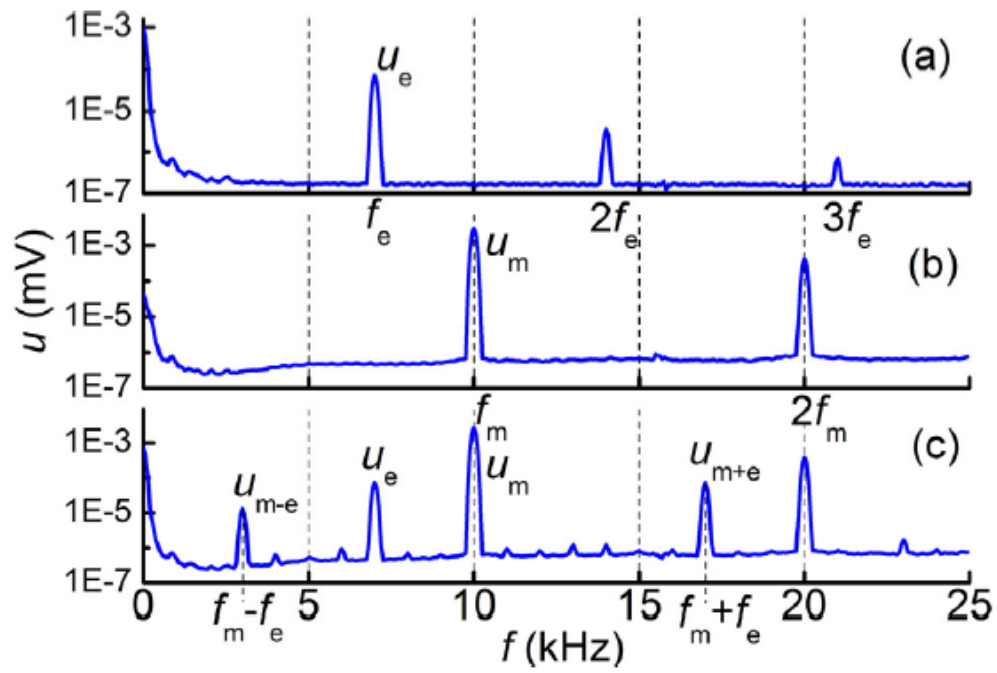
Fig. 3. Frequency spectra of the voltage generated by Metglas-PZT heterostructure when excited by: (a) magnetic field, (b) electric field, (c) magnetic and electric fields at the same time. Bias magnetic field is $H = 13$ Oe.
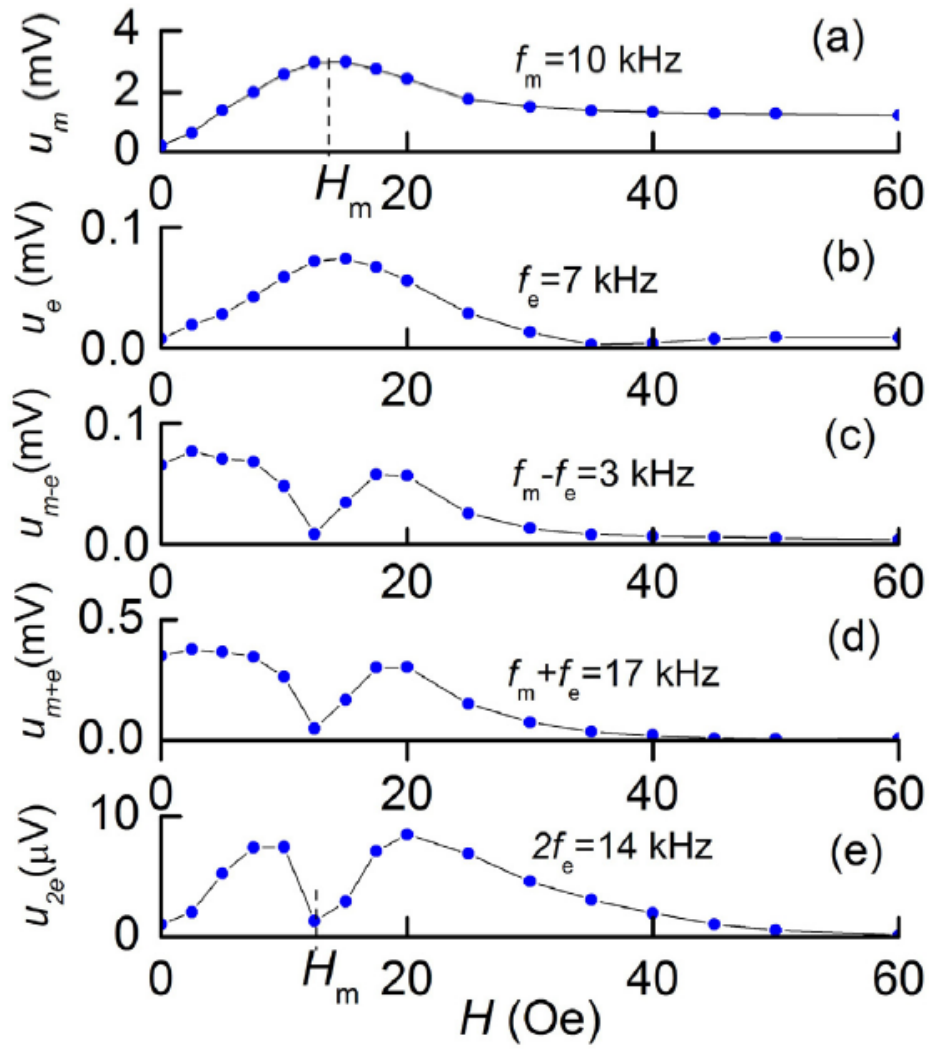
Fig. 4. Amplitudes of spectral components of voltage response versus bias magnetic field H in the case of simultaneous excitation of the heterostructure by magnetic ($h=1$ Oe, $f_m = 10$ kHz) and electric ($e = 100$ V/cm, $f_e = 7$ kHz) fields.
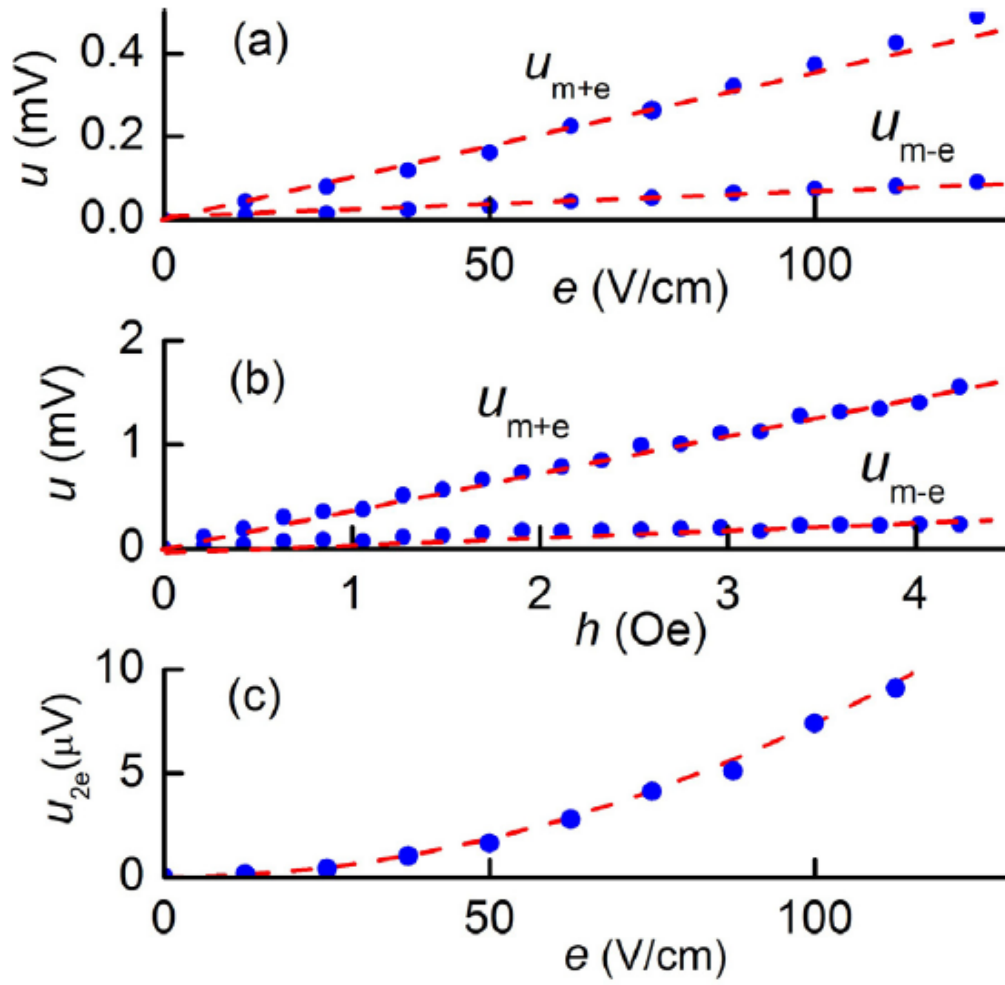
Fig. 5. Dependences of amplitudes of harmonics with difference and sum frequencies on: (a) amplitude of electric field e for $h = 1$ Oe and (b) amplitude of magnetic field h for $e = 100$ V/cm and $H = 3$ Oe. (c) The amplitude of the $2f_e$ harmonic versus amplitude of electric field e for $H = 7.5$ Oe.
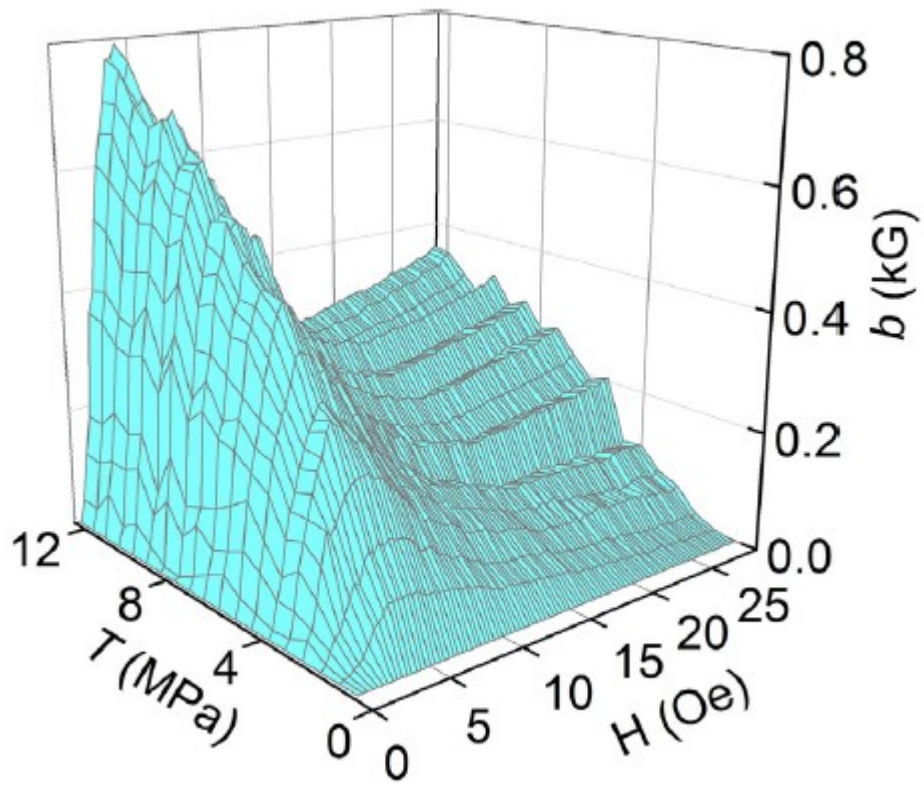
Fig. 6. Dependence of inductance L of the coil loaded with the FM tape on bias magnetic field H for different mechanical stresses T.
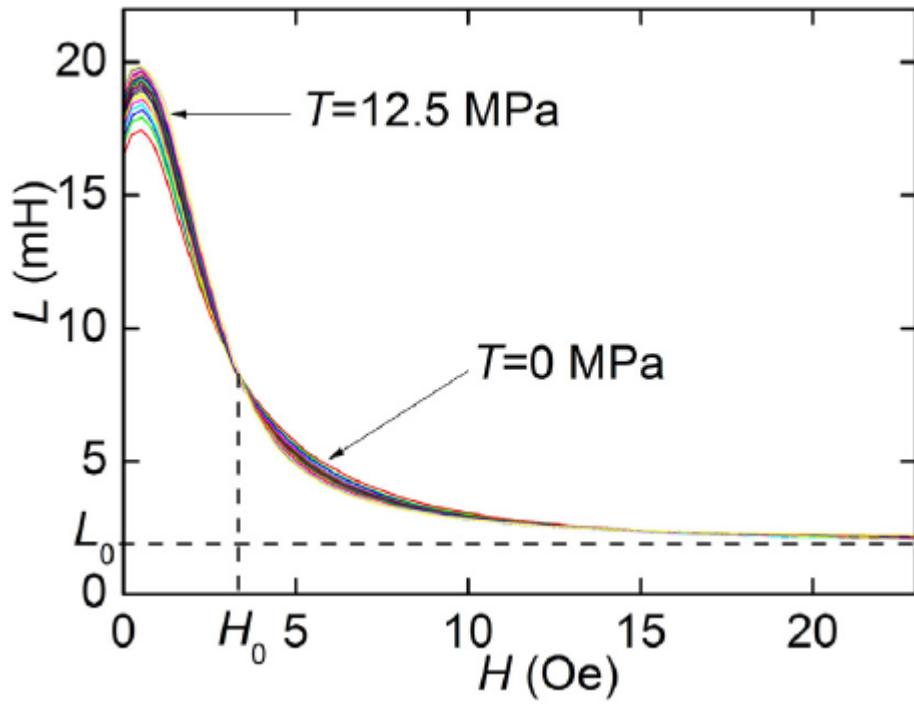
Fig. 7. Magnetic induction b in the Metglas layer as a function of magnetic field H and mechanical stress T.

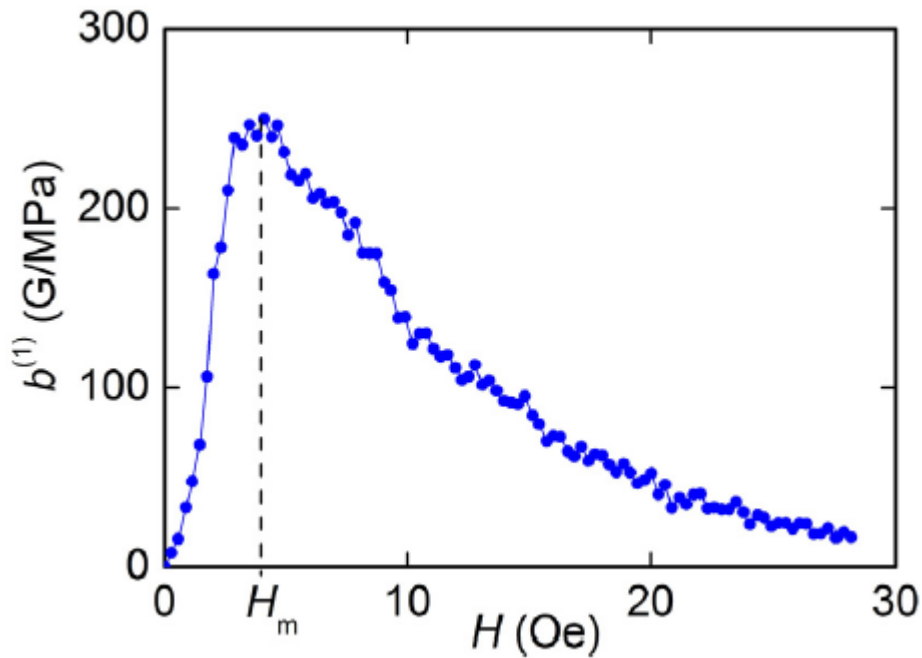Fig. 8. Dependence of linear elastomagnetic coefficient $b^{(1)}$ on magnetic field H for Metglas tape for low mechanical stresses ($T \approx 0$).